Review paper of Improvement of Mechanical Properties of Hybrid Metallic and Ceramic Reinforced Aluminium Composites Material (Al+Ti+MA)

Alok Pradhan[1] Purshttom Prajapati[2] Mayur Thombre[3]

[1,2,3]Department of Mechanical Engineering

[1,2,3]Shri Shankaracharya Institute of Technology & Management Junwani Bhilai, India

Abstract— In the present examination, the joined Ti (miniaturized scale) and Al2O3 (small scale or nano) particles fortified economically unadulterated Al lattice composites have been created through powder metallurgy course. An itemized microstructural portrayal and the assessment of mechanical properties including wear and erosion conduct have been done. As a reason for examination, the equivalent has been researched for the Al composites fortified with these particles alone.The various combinations were Al+8%Ti (Al+Ti), Al+8%micro-Al2O3 (Al+MA), Al+8%nano-Al2O3 (Al+NA), Al+8%Ti+8%micro-Al2O3 (Al+Ti+MA) and Al+8%Ti+8%nano-Al2O3 (Al+Ti+MA) (all vol.%).

Keywords: Mechanical Properties of Hybrid Metallic, Specimen fabrication, Ceramic Reinforced Aluminium Composites Material

I. INTRODUCTION

Al and Al alloys became attractive candidate for the application in aerospace, defence and automotive industries owing to their versatile properties. A major requirement for such applications is the high strength along with reasonable ductility. There has been a constant effort to enhance the mechanical properties of Al alloys by alloying additions, heat treatment, thermo-mechanical processing, severe plastic deformation (SPD) and so on. However, these methods have their own limitations which are difficult to overcome. For example, many SPD processes produce relatively small quantities of material and therefore, it is very difficult to produce large quantities of materials at low cost. The development of the metal matrix composites (MMCs) is a well-accepted method to improve the strength of metals and alloys. In the race for production of MMCs, aluminium metal matrix composites (AMMCs) received particular attention in the automobile and aerospace industries as potential advanced structural materials in the past three decades owing to their high specific strength, stiffness, superior wear resistance, excellent elevated temperature resistance and the widespread availability of the low cost fabrication techniques [1-5]. The continuous fibre reinforced AMMCs are ruled out owing to their high cost, the whiskers are not preferred due to health hazards and the short fibre reinforced AMMCs exhibit anisotropic properties. Therefore, the Al based particles reinforced composites having low density, good formability and isotropic properties have to be developed. The AMMCs reinforced with the popular ceramic particles like SiC, Al2O3, TiO2, AlN, B4C and TiC [6] exhibit the beneficial effect of superior strength, however, suffer from the serious disadvantage of low ductility [7-10]. The reduction in ductility arises owing to the brittle interfacial reaction products, poor wett ability, particle clusters as well as the presence of porosity and de-bonding at the particle–matrix interface. There have been a few recent investigations on the composites reinforced with hard metallic particles [11-17] that exhibited reasonable good ductility. Therefore, an alternative approach in the step of designing composites would be to take the simultaneous advantage of ductility from the addition of metallic reinforcement as well as the strength from the addition of hard ceramic particles. The composites reinforced with both metallic as well as ceramic particles are expected to exhibit a good combination of strength and ductility.

Titanium is an attractive choice as reinforcement owing to its high specific strength, high stiffness, good fatigue properties, good creep and high temperature oxidation resistance [12]. In the present investigation, Ti particles (macro) and Al2O3 particles (macro and nano) reinforced Al matrix composite have been processed via powder metallurgy route. A detailed micro structural as well as mechanical, wear and corrosion characterizations have been carried out.

II. LITERATURE SURVEY

A. MMCs reinforced with metallic particles:

Hassan and Gupta explored the natural titanium molecule strengthened magnesium orchestrated utilizing broke down dissolve affidavit method pursued by hot expulsion. They inferred that the expansion of titanium as fortification insignificantly improves the dimensional soundness of unadulterated magnesium. The nearness of titanium fortification prompted an improvement of 0.2% yield quality and pliability while the UTS were unfavorably influenced. They watched the molecule breakage was the commanding support related disappointment component under malleable stacking [29]. Hassan and Gupta in another examination incorporated the basic Ni fortified Mg utilizing an imaginative broke down dissolve statement procedure pursued by hot expulsion. Microstructural portrayal of the composite demonstrated uniform dissemination of Ni particles in the grid, great interfacial honesty of magnesium lattice with nickel particles and Mg-Ni based intermetallics, and the nearness of negligible porosity. Physical properties portrayal uncovered that expansion of nickel as support improves the dimensional soundness of unadulterated magnesium. Mechanical properties portrayal uncovered that the nearness of nickel fortification lead to huge improvement in hardness, versatile modulus, 0.2% yield quality and UTS while the malleability was antagonistically influenced. The outcomes further uncovered that the mix of0.2% yield quality, UTS, and pliability displayed by nickel fortified magnesium stayed much better notwithstanding when looked at than high quality magnesium amalgam AZ91 strengthened with a lot higher volume level of SiC [30]. Wong et al. [31] detailed the fruitful handling of nano-sized Cu particles

fortified Al composites utilizing powder metallurgy method joining microwave helped two-directional sintering. The sintered examples were hot expelled and described as far as physical, microstructural and mechanical properties. Microstructural portrayal uncovered negligible porosity and the nearness of a consistent Network of nano-measure Cu particles and Mg2Cu intermetallic stage decorating\the molecule limits of the metal grid. Coefficient of warm extension estimation of magnesium network was improved hardly with the expansion of nano-measure Cu particles. The expansion of nano-estimate Cu particles lead to an expansion in hardness, versatile modulus, 0.2% yield quality (YS), extreme elasticity (UTS) and work of break of the lattice [31]. Thakur and Gupta first built up the Al based composite fortified with Ti particles created by utilizing the crumbled dissolve statement (DMD) preparing strategy pursued by hot expulsion. Microstructural portrayal of the as-expelled composite examples uncovered a close uniform dispersion of the Ti particles in the Al grid, great interfacial respectability between the Ti particles and the Al framework and negligible nearness of porosity. The expansion of Ti particles brought about an increment in macrohardness, 0.2% YS, UTS and versatile modulus. Be that as it may, the pliability of the composite was observed to be diminished by the expansion of Ti particles in the Al framework. The cracked examples of the composite demonstrated the bendable method of break on account of Al lattice while molecule crack and debonding were seen as the disappointment method of the Ti support [32]. A test examination was performed to anticipate stream bends, dynamic recrystallisation conduct of AZ91magnesium/titanium metal network composite dependent on result from hot pressure test. The pressure tests were done in a temperature scope of 300°−500°C and at a strain rate scope of 0.001−1 sec-1 and the stream bends were gotten. The handling guide of the concentrated material was gotten by following the dynamic material model. Microstructural portrayal studies directed on the compacted composite examples utilizing optical and examining electron microscopy, uncovered unique recrystallization, debonding of Ti Particles, molecule breakage, and stream confinement. The perceptions were performed so as to portray the conduct of the material under hot shaping activity as far as material harm and small scale auxiliary alteration [33]. Another bimetal magnesium/aluminum (Mg/Al) macrocomposite containing mm-scale Alcove Reinforcement was created through throwing and hot coextrusion. Portrayal uncovered genuinely uniform Al volume part along the expelled pole length owing to mechanical interlocking between Mg shell and Al center. Real deformities were missing and Mg–Al interfacial honesty was great. Warm solidness of the macrocomposite was imperceptibly improved when contrasted with unadulterated Mg. Results uncovered that the nearness of the Al center prompts a diminishing in quality of Mg, however an improvement in firmness just as huge increment in disappointment strain (144%) and work of crack (73%) of Mg. An endeavor is made in the present examination to explore the impact of quality of mm-scale Al center on the microstructure and mechanical properties of the bimetal Mg/Al macrocomposite [34]. Yadav and Bauri [4,5] created the Ni molecule inserted aluminum framework composite by rubbing blend preparing (FSP). The FSP came

about uniform scattering of nickel particles in the aluminum framework with amazing interfacial holding and grain refinement of the grid. The composite showed triple increment in the 0.2% confirmation worry with holding a considerable measure of malleability. Wu et al. [35] examined the impact of Mo expansion on the microstructure and wear opposition of in-situ TiC/Al composite utilizing a throwing course helped without anyone else engendering high-temperature union. The exploratory outcomes displayed that the Mo improves the wettability among TiC and aluminum dissolve because of the development of a Mo-rich shell around the TiC particles. When contrasted with the non-Mo included composite, the expansion of 1.0 wt% Mo created better grid structure, huge refinement and uniform circulation of TiC particles in the network. It is likewise announced that both wear and pliable properties of TiC/Al composite were improved with 1.0 wt % Mo expansion. Be that as it may, the further increment of Mo substance decays the properties attributable to the development of delicate Al5Mophase

B. MMCs reinforced with nano ceramic particles:

Wang et al. manufactured in situ 100-200 nm Al2O3 particles fortified Al composites by direct dissolve response process. They watched the in situ created Al2O3 molecule shaving different unpredictable shapes scatter consistently in the network with the perfect interface among molecule and grid. They watched high thickness of disengagements produced broad fine subgrains around the Al2O3 particles and reasoned that the composites are completely reinforced by Al2O3 particles, yet in addition by the high thickness separations and fine subgrains [36]. Mazahery and Ostadshabani consolidated alumina nanoparticles into the A356 aluminum amalgam by a mechanical stirrer and barrel shaped examples were thrown. A uniform circulation of fortification, grain refinement of aluminum grid, and nearness of the negligible porosity was seen by microstructural portrayal of thecomposite tests. Portrayal of mechanical properties uncovered that the nearness of nanoparticles fundamentally expanded compressive and ductile stream worry at both throwing temperatures. It was uncovered that the nearness of nano-Al2O3 support prompted noteworthy improvement in 0.2% yield quality and extreme elastic pressure while the flexibility of the aluminum framework is held. Fractography examination demonstrated moderately malleable crack in pliable broke examples [37]. Su et al. [5] manufactured the nano Al2O3/2024 composites by strong fluid blended throwing joined with ultrasonic treatment. The composite showed fine grain, sensible Al2O3 nanoparticles conveyance in the framework, and low porosity. Strong fluid blended throwing system was viable in hindering the agglomeration of nanoparticles in the network. The utilization of ultrasonic vibration on the composite dissolve duringthe hardening not just refined the grain microstructure of the framework, yet in addition improved the dissemination of nano-sized fortification. Contrasted and the lattice, a definitive rigidity and yield quality of 1 wt% nano-Al2O3/2024 composite were upgraded by 37%and 81%, separately. The better ductile properties were credited to the uniform dissemination of support and grain refinement of aluminum grid [5]

C. MMCs reinforced with both micro and nano ceramic particles:

The impacts of the expansion of Al2O3 molecule fortifications of various sizes (5 vol% every one of small scale and nano) on the microstructure, physical and mechanical properties of magnesium based composite was examined by Wong et al [38]. Powder metallurgy including microwave helped quick sintering method was received as the blend course. Negligible porosity was seen in every one of the examples. The mechanical properties like hardness, flexible modulus,0.2% yield quality, extreme rigidity demonstrated a discernible increment on expansion of micron and nano-sized molecule fortifications in magnesium grid, though the malleability to some degree diminished when contrasted with unadulterated magnesium. At the point when nano-sized alumina particles were utilized from 0.5 to 0.75vol%, there was an expansion in versatile modulus and malleability, while no consequent changes in other mechanical properties. Be that as it may, as the vol part came to 1%, an improvement was seen in practically all properties. Sajjadi et al. [39] utilized composting to manufacture aluminum–lattice composite strengthened with small scale and nano-alumina particles. The microstructure of the composite uncovered that utilization of composting procedure prompted a change of a dendrite to a nondendritic structure of the lattice compound. The SEM micrographs uncovered that Al2O3 nano particles were encompassed by silicon eutectic and slanted to advance toward between dendritic districts. They were scattered consistently in the network when 1, 2 and 3 wt.% nano Al2O3 or 3 and 5 wt.% small scale Al2O3 was included, while, further increment in Al2O3 (4 wt.% nano Al2O3 and 7.5 wt.% miniaturized scale Al2O3) prompted agglomeration. The thickness estimations demonstrated that the measure of porosity in the composites expanded with expanding weight portion and speed of mixing and diminishing molecule measure. The hardness results demonstrated that the hardness of the composites expanded with diminishing size and expanding weight division of particles [39].

D. MMCs reinforced with both metallic and ceramics particles:

In one of the examination investigation of Q.B. Nguyen and M. Gupta [40], various measures of Ca (1 wt. %, 2 wt. % and 3 wt. %) were joined into an AZ31B/nano-Al2O3 magnesium amalgam composite utilizing the broke down dissolve affidavit (DMD) strategy pursued by hot expulsion. The examples were portrayed as far as physical, microstructural and mechanical properties. Microstructural portrayal studies uncovered that with expanding Ca expansion, the lattice grain measure and the nearness of Mg17Al12 stage decreased. Despite what might be expected, it was seen that the nearness of Al2Ca stage expanded. Moreover, the nearness of Ca altogether helped with improving 0.2% yield quality (YS) and extreme elasticity (UTS) while disappointment strain (FS) was decreased. An endeavor is made to relate the impact of expanding measure of Ca on the microstructure and mechanical properties of AZ31B/nano-Al2O3 composite [40]. Once more, Q.B. Nguyen and M. Gupta blended a half breed AZ31B combination based composite by utilizing a hardening handling course [41]. Be that as it may, for this

situation, alongside the nano-alumina particles, copper was included as a metallic fortification. The association of the team prompted an improvement in microstructural qualities (decreased interparticle separating), dimensional soundness, hardness and in general malleable reaction of AZ31B. In the event of AZ31B–Cu–Al2O3 tests there was blended sort crack with restricted nearness of micro crack though, AZ31B–Cu tests exhibited noteworthy nearness of micro cracks and the breakage of Cu particles. It tends to be inferred that these kind of combination composite (half and half; metallic+ceramic fortifications) can exceed expectations in different designing applications when contrasted with AZ31B or AZ31B–Al2O3 nanocomposites. Comparative kind of conduct was seen in a nano-composites (AZ31B–3.3Al2O3–Cu) based onmagnesium compound AZ31B, created utilizing DMD technique [42]. Here, notwithstanding the majority of the properties referenced in the over two cases, the compressive quality additionally increment with increment.

III. OBJECTIVE OF THE PROJECT

The Main objective of the proposed project is
1) Study of Improvement of Mechanical Properties of Hybrid Metallic and Ceramic Reinforced Aluminium Composites Material (Al+Ti+MA).
2) Study of grain refinement in the Al+NA and Al+Ti+NA composites may have added to the improved consumption obstruction.
3) The particles can be considered as deformities in the aloof film. In this manner, it is difficult to build dense passive layer free from defect increase of the composites re in forced with higher volume portion of clay and metallic particles.
4) Detriment land may cause different ceil corrosion resistance among the composites thought is unimaginable to separate them

IV. METHODOLOGY & EXPERIMENTAL PROCEDURE

A. Specimen fabrication

1) Raw materials:
For this research we had chosen commercially available pure aluminum of purity >98% and particle size 50µm as our matrix. Titanium of microns and alumina (both in nano and microns) were used as thereinforcements.

2) Blending:
To begin with the powder metallurgy method, we first blended the powders in right proportion. The blending process was carried out in Abrasion Tester for 2 revolutions. Titanium and alumina both were added in same 8 vol% with matrix pure aluminum differently to get five distinct combinations.

Materials used	Abbreviated nomenclature
Al–Macro Ti particles	Al+Ti
Al–Macro Al2O3 particles	Al+MA
Al–Nano Al2O3 particles	Al+NA
Al+Ti+Macro Al2O3 particles	Al+Ti+MA
Al+Ti+Nano Al2O3 particles	Al+Ti+NA

Table 3.1: Various combinations of the Ti and Al2O3 particles in the composites and their corresponding abbreviated nomenclature

3) Compaction:

Following the blending of the powders, the green compact of 15mm diameter was produced in an electrically operated uni-axial cold compaction machine at an applied pressure of 600MPa. The aspect ratio (l/d) of 15mm dia pellets was maintained at 0.8 as per ASTM- E09 standards. For this purpose a stainless steel die of internal diameter of 15mm was used. The wall of the die was properly lubricated by zinc stearate. After every compaction, the system was kept in hold for 2min to reduce the anti-effects of the back-pressure produced.

4) Sintering:

The sintering of the green compacts was carried out in a tubular furnace underargon atmosphere. First of all the tube was evacuated to a vacuum level of 10-5bar and the samples were placed on a crucible inside the chamber. Then Ar gas was supplied at 200ml/min so that no oxidation takes place during sintering, since Aluminium is very much prone to get oxidized. Four samples of each of the combinations mentioned in table1 were sintered at 600°C for 120min. On completion of sintering, all samples were left to cool down to room temperature inside the furnace itself before exposing it to outsideatmosphere.

B. Specimen characterization

1) XRD analysis:

In order to study the phases present in the specimen, X-ray diffraction (PANalytical model: DY-1656) was done using CuKα (λ=1.5418A°) radiation. The scanning range used for the diffraction was 10°- 90° with a step size of 2°/min.

2) Scanning Electron Microscopy (SEM) observation:

The microstructure was characterized by scanning electron microscope (JEOL 6480 LV). We used Keller's reagent (1.5%HCl, 1%HF, 2.5%HNO3 and rest distilled water) for etching the specimen. 20kV was maintained as the accelerating voltage for all of the micrographs. Here we concentrated on how the particles were distributed, interface bonding between reinforcement particle and matrix, grain size, etc. The samples after wear and corrosion tests were also visualized under SEM.

3) Density measurement:

Theoretical density was estimated on the basis of rule of mixtures. ρcomposite = (ρAl× vol% of Al) + (ρreinforcement× vol% of reinforcement) where, the second term 'reinforcement' on the R.H.S of the above equation denotes to either of the earlier mentioned combinations (table 1). The sintered density was measured by Archimedes Method. The weight of the pellets were first measured in air and then in distilled water. Contech CB series analytical balance with a density measurement kit package from Contech was used for the density measurements.

4) Hardness measurement:

The micro hardness was measured on the polished surface of the specimen by the help of Vickers hardness tester (Leco Micro hardness Tester LM248AT). The indentation was made by a load of 100gf with a dwell time of 10secs. For each of the sample, eight readings were taken considering the average of their values as the hardness of the same.

5) Wear tests:

Wear tests were completed in dry sliding condition as per the ASTM G-99 standard utilizing a stick on-plate wear and rubbing screen model no. DUCOM;TR-20-M100. The machine comprises of an EN32 steel plate having a hardness estimation of HRC 58 and measurement of100 mm.The cylindrical specimens of 6 mm diameter and 12 mm height were machined. Wear tests were completed at the typical heap of 30 N. Every one of the tests were done at a fixed separation of 100 mm from the focal point of the plate at 300 rpm, comparing to a straight speed of 1.57 m/s for a steady sliding separation of 1.0 km. During the wear test, the stature loss of the example was ceaselessly observed and it was changed over to volume misfortune (in mm3) by increasing it with the cross-sectional region. The wear rate (in mm3/m) was acquired by partitioning the volume misfortune with the sliding separation (in m). When each test, both the circle and the examples were cleaned altogether with CH3)2CO and afterward dried so as to stay away from tainting. Each test was done at any rate twice so as to check the reproducibility and normal estimation of the tests was taken to decide the wearrate.

6) Compression tests:

The compressive strength of the composite was measured in a universal testing machine (Instron- SATEC series servo-hydraulic machine) at a crosshead speed of 0.5mm/min. The nominal diameter and height of all samples tested were 15 and 12 mm, respectively as per the ASTM E9-89 standard.
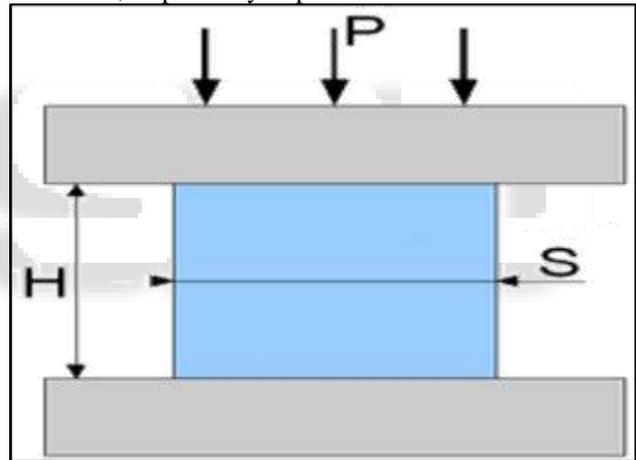

Fig. 3.1: Load application during uni-axial compression test.

7) Corrosion tests:

Corrosion tests were performed on all the specimens after slightly grinding the surfaces with silicon carbide paper (2500 grit, deionized water cooling). Finally, all the specimens were cleaned in alcohol prior to corrosion test. Electrochemical corrosions tests were carried out in aqueous 3.5 wt.% NaCl solution saturated with atmospheric oxygen and adjusted to neutral pH using NaOH with an exposed area of 0.5 cm2 using a Gill AC potentiostat/galvanostat. The corrosion cell (333 ml) with a typical three electrode set-up, with the specimen as the working electrode, a saturated Ag/AgCl electrode as reference electrode and a platinum mesh as counter electrode was used. The electrolyte temperature was controlled at 22± 0.5°C and the electrolyte was stirred during the experiments. One experiment lasted for about 19 hours and consisted of three subsequent tests as follows.

1) Recording of the free corrosion potential for 5 minutes.
2) Potentiodynamic polarization scans starting from −150 mV relative to the free corrosion potential with a scan rate of 0.2 mV/s. The test was terminated when a

corrosion current density of 0.1 mA/cm2 was exceeded to minimize the damage on the specimen surface before the next sequence started. This test lasted for about 30 minutes. From the cathodic branch of the polarization curve the corrosion rate was determined using the Tafelslope.

3) Subsequently, Electrochemical Impedance Spectroscopy (EIS) estimations at free consumption potential were done utilizing a Gill AC over the recurrence extend from 10 kHz to 0.01 Hz. The sufficiency of the sinusoidal sign was 10 mV. The EIS outputs were led at the interim of 3, 6, 9, 12, 15 and 18 hours of inundation. The charge move opposition was determined from the convergences of the hover with the genuine axis(0°phaseshifts)giving the arrangement obstruction and the entirety of the solution and the charge transfer resistance respectively (assuming a simple Randles circuit model).After the corrosion tests, the specimens were ultrasonically cleaned and observed under microscope..

V. RESULTS AND DISCUSSION

A. Synthesis

Pure Al and its composites were successfully synthesized using powder metallurgy technique coupled with conventional sintering technique. The results of the characterization studies performed on the materials clearly indicate the feasibility of using conventional sintering to develop Al composites.

B. Density and porosity

Table 4.1 shows the density and porosity measurement values for all the Al-based composites. It can be seen that the density values increased with the addition of both metallic and ceramic particles as compared to that of pure Al (density 2.7 g/cc). The increase in density for the Al+Ti composite is more as compared to that of the composites reinforced with macro and nano-sized Al2O3 particles. There is a difference between the experimental density and the theoretical density values. This indicates the porosity present in allthe composites is significant, which is the characteristics of the materials processed via powder metallurgy technique with conventional sintering. It is also true that in the present investigation no secondary processing (like extrusion) was carried out, which generally reduce the existing porosity to some extent. It is also observed that the porosity level is reduced in case of the composite reinforced with macro-sized Al2O3 as compared to the composite reinforced with nano-sized Al2O3. The similar trend in porosity results i.e., decrease in porosity per cent with increase in particle size was also observed earlier by Sajjadi et al. in the A356 alloy composites reinforced with macro and nanoAl2O3 and processed by compocasting [39]. The results also exhibited an increase in the density with increase in the total content of Ti and Al2O3 in the Al matrix. This can be attributed to higher density of Ti (4.507 g/cm3) and Al2O3 (3.95 g/cm3) particles as compared to that of pure Al (2.7 g/cm3)matrix.

S. No.	Material	Experimental density (g cm³)	Theoretical density (g cm³)	Porosity (%)
1	Al-Ti	2.7783	2.8445	2.33
2	Al-NA	2.7120	2.8000	3.14
3	Al+MA	2.7416	2.8000	2.08
4	Al-Ti-NA	2.8643	2.9500	2.90
5	Al-Ti-MA	2.8758	2.9500	2.52

Table 4.1: Results of density and porosity measurements for the Al-based composites

C. XRD Analysis

Fig.4.1 shows the X-ray diffraction patterns for all the fabricated Al-based composites. The experimental data obtained were compared with that of the standard powderdiffraction results for Al, Ti, Al2O3 and Al3Ti intermetallic phases. It is evident that all the composites exhibited peaks corresponding to pure Al along with the peaks corresponding to pure Ti in case of Al+Ti; Al2O3 in case of Al+NA and Al+MA; Ti and Al2O3 in case of Al+Ti+NA and Al+Ti+MA composites. Apart from these phases, few peaks corresponding to the intermetallic phases Al3Ti are also present in the Al+Ti, Al+Ti+NA and Al+Ti+MA composites, which are produced by the reactions of Al with Ti. The studies conducted so far have shown that the addition of Ti in the Al leads to a reaction between Ti and Al to form Al3Ti through peritectic reaction. The interaction between Ti and Al results in either a solid solution of Ti in Al (with a very limited solid solubility) or the formation of Al3Ti through peritectic reaction [43]. The microstructures of Al–Ti synthesized by using conventional casting with slow cooling rate, spray atomization and deposition with reasonably high cooling rates revealed the as-expected existence of Al3Ti inter metallic phase. Thus, the inter metallic phase Al3Ti, which is present in Al-Ti system, is not beneficial for the development of composites. The formation of the intermetallic phase Al3Ti in the Al-Ti system has also been reported by several researchers.
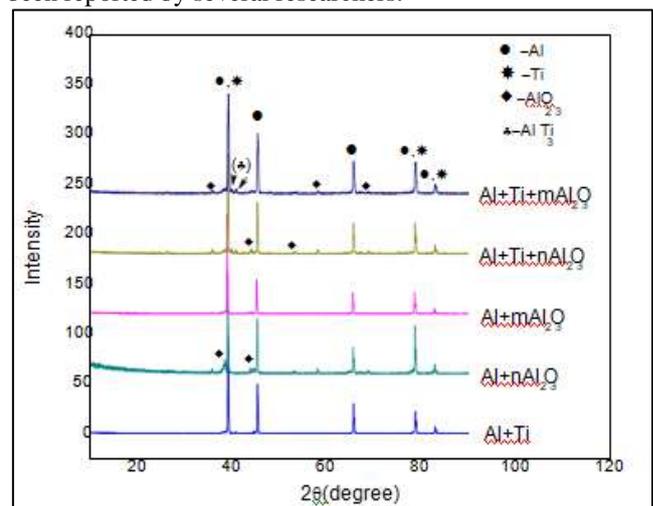

Fig. 4.1: X-ray diffraction patterns obtained from all the Al-based composites

D. Microstructure

(a)   (b)

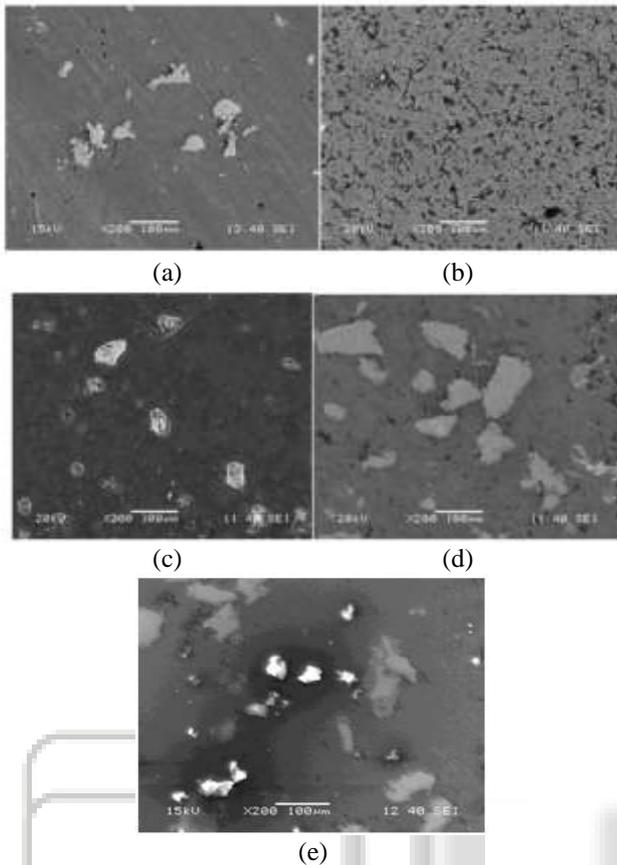(c)   (d)

(e)

Fig. 4.2: Representative as sintered SEM micrographs for all the Al-based composites corresponding to: (a) Al+Ti; (b) Al+NA; (c) Al+MA; (d) Al+Ti+NA and (e)Al+Ti+MA.

Fig. 4.2 (a-b) shows the SEM micrographs obtained from the as-received Ti and Al2O3 powders. It is evident that there is no significant difference in grain size and appearance of the Ti powder and the same is true for the Al2O3 power as well. Fig.4.2 (a-e) shows the representative microstructures for all the composites. The micrographs revealed the presence of porosity in all the composites and the extent of porosity present is more in case of the composites reinforced with nano-sized Al2O3 (Fig. 4.2 (b and d)) alone. This is also supported by the experimental porosity results obtained using density measurement as shown in Table 4.1. It is evident from Fig. 4.2 (a,d,e) that the metallic Ti particles were uniformly distributed in the Al+Ti,Al+Ti+NA and Al+Ti+MA composites .However, the inter metallic 1phase (Al3Ti) formed owing to the metallic addition was not observed in the representative micrographs (Fig. 4.2 (a,d,e)) taken at low magnification. There is no nano-Al2O3 particles agglomeration in the composites, as observed in the BSE image (Fig. 4.3).Therefore, the clustering of the reinforcing particles in general is negligible in all the composites employed. The interfacial respectability was evaluated as far as interfacial debonding and the nearness of micro voids at the interface. The micrographs of the composites showed great interfacial uprightness between the network and the fortifications. The nonattendance of debonding or intermittence at the interface demonstrated unrivaled sintering. The micrographs likewise uncovered no interfacial response (at the interface of Ti/Al-network and Al2O3/Al

lattice) for every one of the composites. The microstructural examination of Al+NA composite displayed the noteworthy grain refinement acquired after the expansion of nano-sized Al2O3 particles. The reduction in grain size after the augmentations of micron-sized Ti and Al2O3 is moderately lower when contrasted with that got with the expansion of nano-sized Al2O3. The consolidated expansion of micron-sized Ti and nano-sized Al2O3 prompts the decrease in grain estimate if there should arise an occurrence of the composite Al+Ti+NA too. The decrease in grain size watched is primarily due to the nano-sized Al2O3 particles going about as destinations for grain nucleation during strong state preparing. Further, the nearness of moderately harder Al2O3 particles hinders grain development, in this way bringing about fine grain estimate. Also, the nearness of nano-sized Al2O3 and Ti in the Al+Ti+NA composite confines the grain development because of its capacity to nucleate Al grains and bringing about a huge decrease in normal grain estimate.
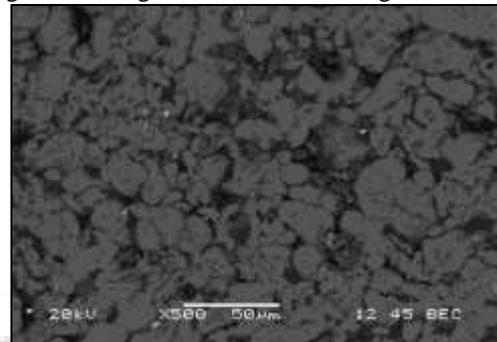

Fig. 4.3: SEM micrograph (in BSE mode) of the composite Al+NA showing minimum agglomeration of nano-Al2O3 particles
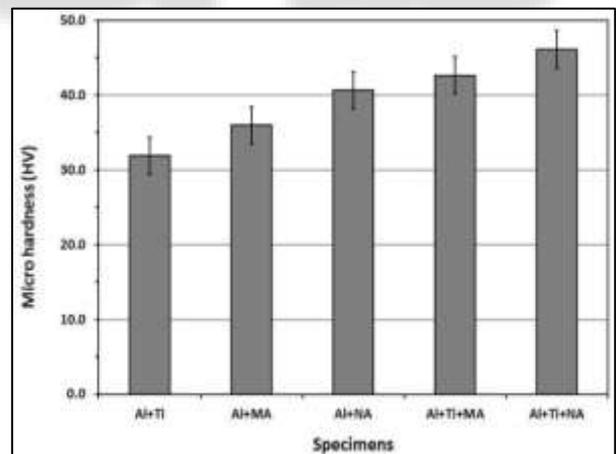
E. Micro hardness

Fig. 4.4: Variation of the average microhardness values for all the Al-based composites

The variation of the average microhardness values for all the composites is shown in Fig. 4.4

It is obvious from the assume that the composites fortified with the artistic particles (small scale or nano) alone shown higher hardness esteems when contrasted with the composite strengthened with metallic particles alone. What's more, the composites fortified with the nano-sized Al2O3 particles alone displayed higher hardness esteem when contrasted with the composite strengthened with the large scale measured Al2O3 particles alone. Further a generally

higher hardness esteems were gotten just when the artistic particles were included mix with the metallic particles (i.e., half and half composites) when contrasted with the composites fortified with the individual particles. Again the Al+Ti+NA half and half composite showed better hardness esteem as thought about than that of the mixture composite Al+Ti+MA. The expansion in hardness of the composites fortified with the Ti metallic particles and nano-sized Al2O3 can be credited fundamentally to (I) an increment within the sight of harder intermetallic stages and nano-Al2O3 clay particles [44] and (iii) the improved grain refinement saw on the Al+Ti+NA composite. This is reliable with prior perceptions made on unadulterated Mg–Cu, AZ91–Cu, and AZ31B–Al2O3 [45-47].

F. Compression behavior

The stress values withstand by all the composites specimens at their 50% reduction of height are reported here.
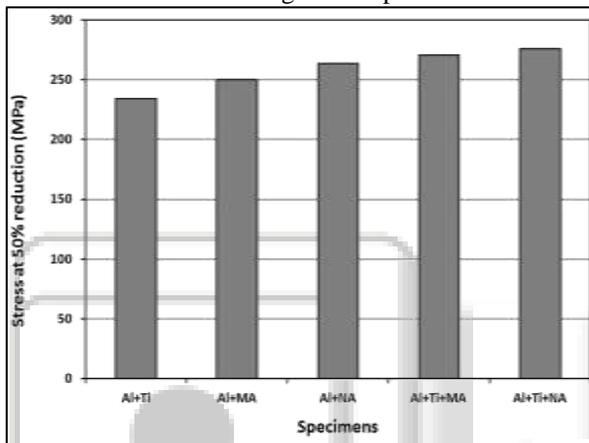

Fig. 4.5: Comparison of the stress values withstand at 50% reduction of the composites

The stress values obtained here (Fig 4.5) is not the ultimate compressive stress but the stress at which the material is reduced to 50% of its initial height. From the plot we can see that the composites fortified with the clay particles (nano) alone supported higher pressure esteems when contrasted with the composite strengthened with metallic particles alone. Also, the composites strengthened with the nano-sized Al2O3 particles alone continued higher pressure an incentive when contrasted with the composite fortified with the full scale estimated Al2O3 particles alone. Further the half breed composites continued higher pressure esteems when contrasted with the composites fortified with the individual particles. Again the Al+Ti+NA cross breed composite continued higher pressure an incentive when contrasted with that of the half and half composite Al+Ti+MA. The expansion in quality of the composites Al+NA and Al+Ti+NA may owe or own reinforcing and grain refinement saw on the nano composites.

G. Dry sliding wear behavior
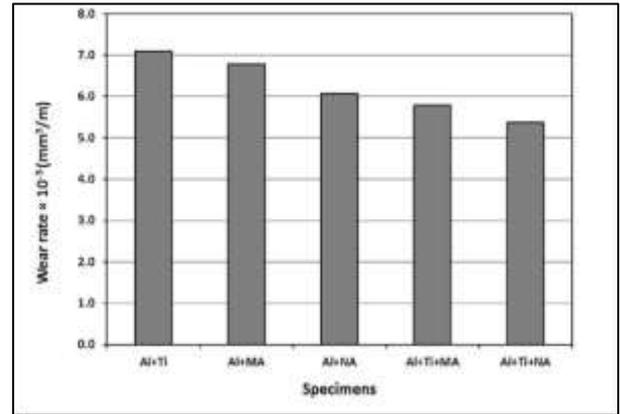
Variation of the volumetric wear rate for the Al-based composites tested using 30 N load and sliding speed of 1.5 m/s.

1) Wear rate

The wear rate in terms of mm3/m at a speed of 1.5 m/s for the all the composites is shown in Fig. 4.6 . It is evident from the figure that the wear rate varies almost in inverse proportion with the hardness of all the composites tested, as generally expected. The wear rate of the composite Al+Ti is the highest among the composites tested at the same load. The composite Al+NA exhibits 10% better wear resistance than the composite Al+MA and the wear rates of both the composites are lower by 14% and 4%, respectively than that of the composite Al+Ti. The hybrid composites which has got higher total volume fraction of reinforcement than the rest of the composites exhibited further decrease in wear rate at the load value employed and it is better than all other composites tested. The Al+Ti+NA hybrid composite exhibit a 7% lower wear rate than the hybrid composite Al+Ti+MA. The lowest wear rate is exhibited by the hybrid composite Al+Ti+NA and it is 24% better than the Al+Ti composite. Thus, the wear resistance increases with the combine addition of metallic and ceramic particles in the Al matrix at the sameload.

2) Observation of the worn surfaces

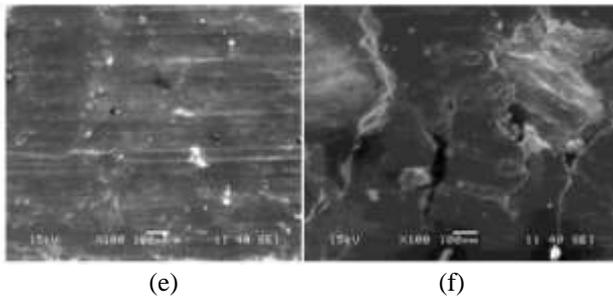(a)   (b)

(c)   (d)

(e)   (f)
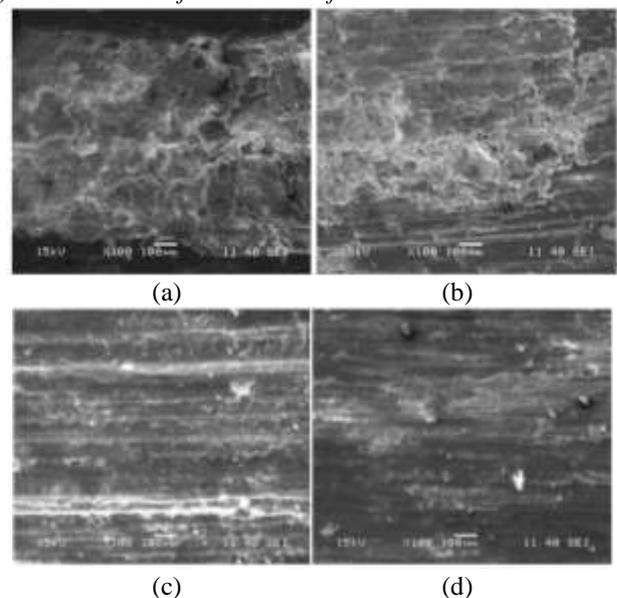
Fig. 4.7: SEM micrographs of the worn surfaces corresponding to the (a) Al+Ti;(b) Al+MA; (c) Al+NA; (d) Al+Ti+MA; (e) Al+Ti+NA and (f) Magnified view of (a)

Fig.4.7 (a-e) shows the micrographs of the worn surfaces of all the composites tested at 30 N load at a sliding speed of 1.5 m/s. Fig. 4.7 (a) shows the worn surface of the Al+Ti composite and the magnified view of the same is shown in Fig. 4.7 (f).It is evident from the figure that the surface is severely damaged and the extensive materials is removed from the surface by delamination, which is a dominant wear mechanism reported for the composites during dry sliding wear test. The micrographs of the worn surfaces of the rest (i.e., Al+MA, Al+NA, Al+Ti+MA and Al+Ti+NA) composites reveal that numerous long continuous and deep grooves had formed on the wear surfaces. These parallel grooves are the proof of micro ploughing and micro cutting and these indicates that the prominent wear mechanism in these composites is abrasion. The worn surface of the Al+MA composite exhibited the most extensive deep ploughing grooves. However, the grooves are relatively shallow and the severity of micro ploughing is progressively decreases on the worn surfaces of the Al+NA, Al+Ti+MA and Al+Ti+NA samples in that order. The severity of the micro ploughing was the lowest on the worn surface of the Al+Ti+NA composite i.e., here the basic wear mechanism remained unchanged and only the grooves became shallow. Careful observation of the worn surfaces revealed some reattachment of wear debris on the worn surfaces and these were the embeddebris.

3) Reason for difference in wear behavior

During sliding wear the stick surface encounters an ordinary connected burden and an extraneous grating power. The subsurface experiences plastic disfigurement bringing about strain slope inside the layer adjoining the contact surface. The size of the strain slope for the most part increments with expanding sliding separation and connected burden [49]. The nearness of strain inclination inside the distorted zone under worn surface is a crucial premise of the event of delamination wear. As indicated by the delamination hypothesis of Suh [48], the plastic disfigurement and disengagement developments at the subsurface district will be periodical during wear. At the point when the disengagement thickness at the subsurface is adequately higher, microcracks are started. The microcracks proliferate parallel to the sliding bearing and blend at the subsurface. At long last the blended splits stretch out to the well used surface with kept sliding. The layer at that point breaks down from the ragged surface producing drop type flotsam and jetsam causing serious wear. The ragged surfaces of the considerable number of composites (aside from Al+Ti) were secured with long persistent depressions parallel to the sliding heading (Fig. 4.7

(b–d)), which are characteristic of grating wear. These sections are predominantly shaped by the furrowing activity of the hard severities present on the solidified steel counter-face or by the caught wear flotsam and jetsam, which are delivered during the sliding procedure in the middle of the mating surfaces, causing wear by expelling little fragments of the material or pushing material into ridges long the sides of the grooves. The sliding wear of aluminum compounds and composites, especially at low burden, is by and large portrayed by the procedure of scraped spot. Some reattachment of wear flotsam and jetsam on the well used surfaces was additionally watched. During the sliding procedure, a piece of the wear flotsam and jetsam, which is delivered because of the sliding contact of two surfaces, was lost from the framework and the rest was stayed in the mating surface. The flotsam and jetsam particles were divided to a fine size during the ensuing sliding. As the garbage become better, its surface vitality increments. It reattaches to the ragged surface because of the Van der Waals power just as the electrostatic force[50].

The delamination wear came about serious basic disturbance and harm of the Al+Ti composite surface. It is realized that when delimitation wear is employable, the material evacuation will be broad and accordingly, the Al+Ti showed the most noteworthy wear rate among the composites tried. Broad furrowing scores were seen on the well used surface of Al+MA composite, notwithstanding, the depressions were moderately shallow and the seriousness of miniaturized scale furrowing was logically diminished on the ragged surfaces of the Al+NA, Al+Ti+MA and Al+Ti+NA tests in a specific order because of the higher hardness estimations of the composite surfaces, which is in charge of lower wear rates of these composites when contrasted with the Al+Ti composite. There have been not many investigations on the impact of kind of fortifications on wear obstruction of composites. Hosking et al. [51] thought about the dry sliding wear conduct of an Al amalgam strengthened either with 20% Al2O3 or 20% SiC particles of a similar size (16 μm). They saw that the SiC particles offered better wear opposition because of the higher hardness than the Al2O3 particles. Along these lines, the Al+MA showed preferred wear obstruction over the Al+Ti composite inferable from the higher hardness of Al2O3 in the present examination. There has been just one examination on the impact of size of molecule fortifications (miniaturized scale (100-200 μm) and nano (47nm))on the wear resistance of Al composites using at herein-on-disk apparatus under dry sliding conditions at a sliding speed of 1.58 m/s for a typical heap of 30 N by Rohatgi et al. [52]. They saw that the nano-composites displayed the best wear execution among the composites researched and hardness of the composites assumed a significant job in improving the wear opposition. Subsequently, the Al+NA composite indicated preferred wear opposition over the Al+MA composite inferable from the higher hardness worth shown by the previous composite in the present examination. Further, the degree of grating wear was most minimal on the ragged surface of the composite Al+Ti+NA inferable from the most noteworthy hardness worth got on it.

H. Electrochemical corrosion behavior

1) Nature of the Corrosion Response

Fig. 4.8 shows the variation of open circuit potential for all the Al-based composites. The estimation of the open circuit potential (or free consumption possibilities) for the 5 minutes of submersion displayed enormous contrasts among the different examples. Clearly the addition of there in for cements (except Tip articles) to the AL matrix shifts the potential to more dynamic qualities, which isn't useful for consumption obstruction. From the beginning of the chronicle free consumption potential the Al+Ti example achieved stable conditions and qualities somewhere in the range of −743 and −765 mV were recorded. This could be ascribed to the latent film development because of the nearness of just Al and Ti in the example and these are known to have magnificent consumption rate. The slants of the two bends relating to Al+MA and Al+NA examples demonstrated a constant drop towards less honorable possibilities, showing nonstop assault on the surfaces of the two examples. The slants of another two bends relating to Al+Ti+MA and Al+Ti+NA half and half composites ended up stable after an underlying shallow drop, showing the underlying assault on the surfaces which was recuperated later on. The open circuit potential measurements after 5minutes of immersion exhibited the noblest potential esteem for the Al+Ti example when contrasted with different examples and enlisted a normal estimation of −755 mV shown in Fig. 4.9.
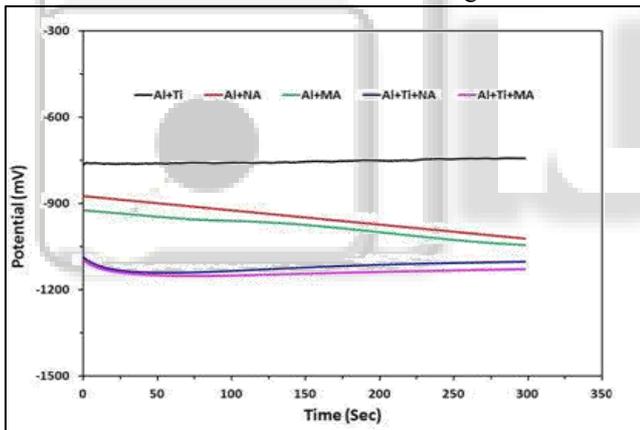

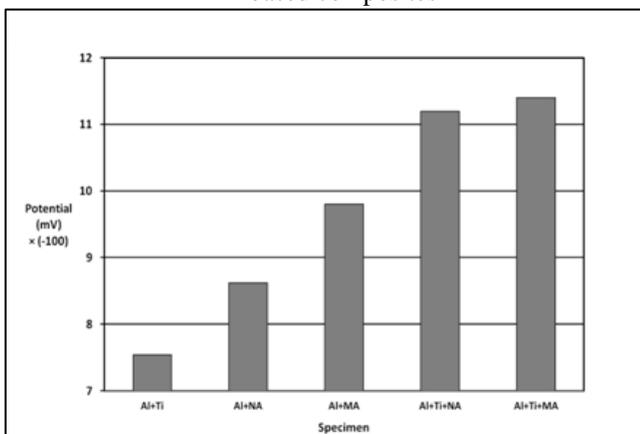Fig. 4.8: Variation of the open circuit potential for all the Al-based composites

Fig. 4.9: Average values of the open circuit potential for all the Al-based composites

VI. CONCLUSION

In the present examination, the joined Ti (miniaturized scale) and Al2O3 (smaller scale or nano) particles fortified monetarily unadulterated Al network composites have been created by means of powder metallurgy course. A nitty gritty microstructural portrayal and the assessment of mechanical properties including wear and erosion conduct have been completed. As a reason for examination, the equivalent has been researched for the Al composites strengthened with these particles alone. The different mixes were Al+8%Ti (Al+Ti), Al+8% micro-Al2O3 (Al+MA), Al+8% nano-Al2O3 (Al+NA), Al+8%Ti+8% micro-Al2O3 (Al+Ti+MA) and Al+8%Ti+8% nano-Al2O3 (Al+Ti+MA) (all vol.%). Following are the ends emerging out of the present study.

1) The composites fortified with the artistic particles (miniaturized scale or nano) alone shown higher hardness esteems when contrasted with the composite strengthened with metallic particles alone. What's more, the composites fortified with the nano-sized Al2O3 particles alone displayed higher hardness esteem when contrasted with the composite strengthened with the small scale measured Al2O3 particles alone. Further the half breed composites Al+Ti+MA and Al+Ti+NA displayed a generally higher hardness esteems and the equivalent was higher for the later composite. The expansion in hardness may owe the grain refinement saw in the Al+NA and Al+Ti+NA composites.

2) The pressure esteems supported by every one of the composites examples in pressure tests during half decrease of their underlying tallness displayed a comparable pattern as hardness.

3) The half and half composites display a superior wear opposition than the composite strengthened with individual sparticleso wing to their higher hardnessas compared to that of the different composites. The overwhelming wear component is seen to be delimitation for the Al+Ti composite and scraped spot for the remainder of the composites.

4) The Al+Ti composite displayed the least consumption rate. The composites strengthened with the artistic particles alone shown higher erosion rate when contrasted with the Al+Ti composite. Furthermore, the Al+NA composites displayed better erosion obstruction when contrasted with the Al+MA composite. Further generally higher consumption rates were shown by the crossover composites. Again the Al+Ti+NA displayed better consumption obstruction as thought about than that of the Al+Ti+MA. The watched grain refinement in the Al+NA and Al+Ti+NA composites may have added to the improved consumption obstruction. Besides, the particles can be considered as deformities in the detached film. Therefore, it is hard to assemble a thick aloof layer free from imperfections if there should arise an occurrence of the composites fortified with higher volume portion of earthenware and metallic particles. All the above highlights are impeding and may cause contrast in erosion obstruction among the composites.

REFERENCES

[1] Miller WS, Humphreys FJ. Scr Metall Mater 25 (1991)33.

[2] Lloyd DJ. Int Mater Rev 34 (1994)1.

[3] Arsenault RJ, Wang L, Feng CR. Acta Metall Mater 39(1991)47.

[4] Pramila Bai BN, Ramashesh BS, Surappa MK. Wear 15 (1992)295.

[5] Kwok JKM, Lim SC. Comp Sci Tech 59 (1999)55.

[6] ASM metals handbook, casting, ASM International, Metals Park, Ohio. 1988: p. 44073.

[7] Fridlyander JN, editor. Metal matrix composites, London: Chapman& Hall,(1995):p.51.

[8] Midling OT, Grong O. Key Eng Mater 104 (1995) 329.

[9] Everette RK, Arsenault RJ, editors. Metal matrix composites: processing and interfaces, Academic Press, Inc. (1991).

[10] Akio K, Atsushi O, Toshiro K, Hiroyuki T. J Jpn Inst Light Metals 49 (1999)149.

[11] Thakur SK, Gupta M. Composites: Part A 38 (2007)1010.

[12] Perez P, Garces G, Adeva P. Comp Sci Tech 64 (2004)145.

[13] Hassan SF, Gupta M. J Alloys Compd 345 (2002)246.

[14] Hassan SF, Gupta M. Mater Res Bull 37 (2002)377.

[15] Hwang S, Nishimura C, McCormick PG. Scr Mater 44 (2001)2457.

[16] Lu L, Lai MO, Toh YH, Froyen L. Mater Sci Eng A 334 (2002)163.

[17] Hassan SF, Gupta M. J Alloys Compd, 35 (2002)10.

[18] Miracle DB. Comp Sci Tech 65 (2005)2526.

[19] Surappa MK. Sadhana, 28 (2003)319.

[20] Yadav D, Bauri R. Mater Sci Eng A 528 (2011)1326.

[21] Yadav D, Bauri R. Mater Let 64 (2010) 664.

[22] Torralba JM, da Costa CE, Velasco F. J Mater Proc Tech 133 (2003)203.

[23] Bonollo F, Ceschini L, Garagnani GL. App Comp Mater 4 (1997)173.

[24] Das T, Munroe PR, Bandyopadhyay S. J Mater Sci 31 (1996)5351.

[25] Lieblich M, Gonza´lez-Carrasco JL, Caruana G. Intermetallics, 5 (1997)515.

[26] Costa CE, Ph.D. Thesis (1998), Universidad Polite´cnica de Madrid,Spain.

[27] Rana RS, Purohit R, Das S. Int J Sci Eng Res 3(2012)

[28] Torralba JM, da Costa CE, Velasco F. J Mater Proc Tech 133 (2003)203.

[29] Hassan SF, Gupta M. J Alloys Compd 345 (2002)246.

[30] Hassan SF, Gupta M. J Mater Sci 37 (2002)2467.

[31] Wong WLE, Gupta M. Comp Sci Tech 67 (2007)1541.

[32] Thakur SK, Gupta M. Comp Part A 38 (2007) 1010.

[33] Raghunath BK, Karthikeyan R, Ganesan G, Gupta M. Mater Des 29 (2008)622.

[34] Paramsothy M, Srikanth N, Gupta M. J Alloys Compd 461 (2008) 200.

[35] Wu Q, Yang C, Xue F, Sun Y. Mater Des 32 (2011)4999.

[36] Wang H et al. In situ fabrication and microstructure of Al2O3 particles reinforced aluminium matrix composites, Mater Sci Eng A 527 (2010)2881.

[37] Mazahery A, Ostadshabani M. J Comp Mater 45 (2011)2579.

[38] Wong WLE, Karthik S, Gupta M. J Mater Sci 40 (2005)3395.

[39] Sajjadi SA etal. J Alloys Compd 511 (2012) 226.

[40] Nguyen QB, Gupta M. Proceeding of the 3rd International Conference on Processing Materials for Properties 2008, PMP III; Bangkok; Thailand; 1 (2009)587-591.

[41] Nguyen QB, Gupta M. Mater Sci Eng A 527 (2010) 1411.

[42] Nguyen QB, Gupta M. J Alloys Compd 490 (2010) 382.

[43] Majumdar A, Muddle BC. Mater Sci Eng A 169 (1993)135.

[44] Zhang Z, Tremblay R, Dube D. Mater Sci Eng A 385 (2004) 286.

[45] Ho KF, Gupta M, Srivatsan TS. Mater Sci Eng A 369 (2004)302.

[46] Hassan SF, Gupta M. Mater Sci Tech 19 (2003)253.

[47] Nguyen QB, Gupta M, Comp Sci Tech 68 (2008) 2185.

[48] Suh NP. Wear 44 (1977) 1.

[49] How HC, Baker TN. Wear 232 (1999) 106. [50] Sahin Y. Wear 223 (1998) 173.

[50] Hosking FM etal., J Mater Sci 17 (1982)477.

[51] Rohatgi PK etal. Int J Aerospace Innovations 3 (2011)153-162